ChemComm

The More the Merrier: Optimizing Monomer Concentration for Supersaturation Controlled Synthesis of Stable Ultra-Small $CsPbBr_3$ Nanocrystals for Blue Emission

Journal:	*ChemComm*
Manuscript ID	CC-COM-01-2024-000163
Article Type:	Communication

COMMUNICATION

The More the Merrier: Optimizing Monomer Concentration for Supersaturation Controlled Synthesis of Stable Ultra-Small $CsPbBr_3$ Nanocrystals for Blue Emission

Received 00th January 20xx,
Accepted 00th January 20xx

DOI: 10.1039/x0xx00000x

Vikash Kumar Ravi*, Zheng Li, Shlok Joseph Paul, Ayaskanta Sahu*

Synthesis of strongly quantum confined and emissive $CsPbBr_3$ perovskite nanocrystals with sizes < 4 nm has proven challenging owing to fast nucleation and rapid growth. In this work, ultra-small blue-emitting (~ 461 nm) $CsPbBr_3$ nanocrystals with an average particle size of 3.2 nm are synthesized via a high-temperature (170 °C) colloidal approach by controlling the supersaturation reaction conditions. Our approach yielded stable nanocrystals with uniform size, shape, and excellent color purity, making them promising for blue light emitting diode applications.

Solution processable inorganic lead halide perovskite ($APbX_3$, A= Cs, X= Cl, Br, I) nanocrystals (NCs) have caught the attention of the research community due to their extraordinary optoelectronic properties like near-unity photoluminescence (PL) quantum yield (QY), narrow full width at half maxima (FWHM < 100 meV), and defect tolerance.[1] Particularly in the field of light emitting diodes (LEDs), these NCs hold a very promising future.[2] Green and red LEDs fabricated with $CsPbX_3$ perovskite NCs with an external quantum efficiency (EQE) of > 20% have already been demonstrated.[3,4] Unfortunately, the development of their blue counterpart which is required for a complete color gamut in LED displays (465- 475 nm = pure blue region and < 465 nm = deep blue region) is seriously lagging with corresponding EQEs currently limited to only < 5%.[5,6] This gap in technology exists primarily due to the lack of stable blue emission from lead halide perovskite NCs which in turn can be associated with the lack of robust synthesis schemes for small (< 4 nm) NCs and associated challenges with material stability.[7]

The hot injection synthesis conducted at temperatures ~ 170 °C using oleic acid and oleylamine as ligands, first reported by the Kovalenko group,[8] is one of the most followed and well-studied routes to prepare $CsPbX_3$ NCs. The reaction is very fast and completes within seconds giving rise to cubic NCs of size ~ 9 nm. Owing to the rapid growth, controlling particle size by tuning reaction time is not an option following this approach. Lower injection temperatures lead to $CsPbX_3$ NCs with smaller sizes but with broader size distribution and shape inhomogeneity.[9] The $CsPbX_3$ NCs synthesis are also reported in literature using supersaturated recrystallization method at room temperature popularly known as LARP (ligand assisted reprecipitation) technique.[10] Small-sized or reduced dimensional NCs have primarily been obtained by tuning the nature of ligands used or the ligand-to-precursor ratio in the reaction mixture.[11–13] Recently Akkerman et al.[14] have shown by changing ligand nature, different sizes of $CsPbX_3$ NCs can be realized in a one-pot synthesis at room temperature. The synthesis of ultra-small NCs including magic sized clusters (MSCs) of $CsPbBr_3$ showing deep and pure blue emission has been reported at the room temperature in the literature.[15–20]

In our current work, we show that by tuning the supersaturation condition, the size of the $CsPbBr_3$ NCs can be controlled without modifying the temperature or changing the ligand nature. The supersaturation that we refer to in the manuscript is not the actual measurement but rather the relative supersaturation compared to the standard synthesis reported by Protesescu et al.[8] which is governed by the monomer concentrations. This approach is especially beneficial for device applications since surface chemistry and post-synthetic modification of oleic acid/oleylamine capped $CsPbX_3$ NCs are well explored and understood. The relative supersaturation condition is controlled by changing the concentration of the reactant precursors while keeping their individual ratio as well as the reaction volume the same. Supersaturation is one of the key steps during the synthesis (crystallization) of NCs that controls the size of nuclei and quality of the NCs. Control over supersaturation has been demonstrated to result in higher crystallinity of the resultant NCs.[21,22] Higher supersaturation results in smaller crystallite sizes as given by the Thomson-Gibbs equation:[23] $\mathbf{\Delta\mu = \mu_l - \mu_c = 2\sigma v/r}$, where $\mathbf{\mu_l}$ and $\mathbf{\mu_c}$ are the chemical potentials of solute in solution and solid crystal respectively. The difference in their chemical potentials, $\mathbf{\Delta\mu}$ is termed as the supersaturation, $\boldsymbol{\sigma}$ is the specific surface energy of a crystal, **v** is the volume and **r** are the crystallite sizes. Also, it is noteworthy that the supersaturation reaction condition can be manipulated to result in high-energy facets of the crystals, which is not easily attainable through simple growth schemes.[24] While this approach has been predominantly adopted for II-VI materials like ZnTe NCs,[25] no studies have focused on using this technique for the halide perovskites. We

Department of Chemical and Biomolecular Engineering, New York university, New York, Brooklyn, 11201, USA
Email: vikashravi07@gmail.com, asahu@nyu.edu
† Electronic Supplementary Information (ESI) available: Experimental details, UV-visible and PL spectra, PL lifetime spectra, TEM images, TGA and NMR spectra.
See DOI: 10.1039/x0xx00000x

demonstrate that the size of $CsPbBr_3$ NCs can be reduced from 9 nm to 3.2 nm by increasing the relative supersaturation condition at a constant temperature, resulting in blue emission. We present one of the first reports on ultra-small sized $CsPbBr_3$ NCs synthesized at high temperatures with stable blue emission at 461 nm.

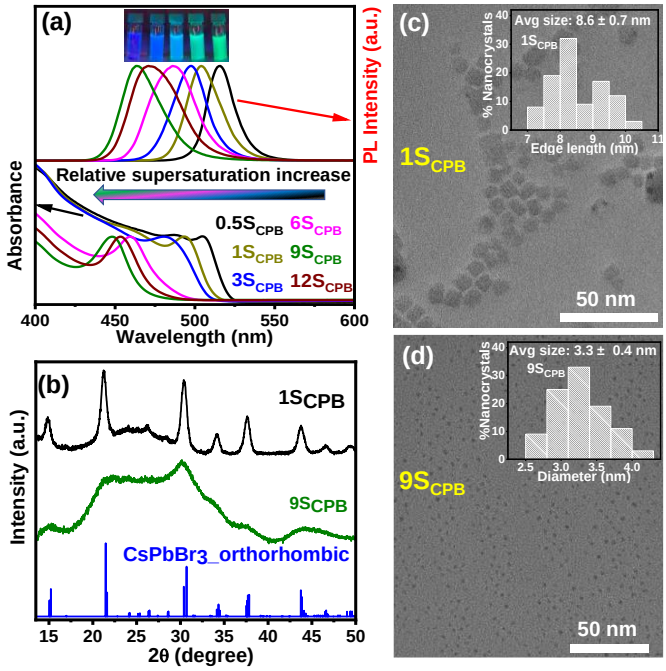

Figure 1: a) Absorbance and PL spectra of $CsPbBr_3$ NCs sample synthesized at 170 °C at different relative supersaturation conditions. It shows with the increase of relative supersaturation, bandgap increases suggesting an increase in quantum confinement and a decrease in size. Inset shows the photograph of the NCs under UV light with different relative supersaturation conditions. (b) PXRD pattern of $1S_{CPB}$ and $9S_{CPB}$ $CsPbBr_3$ NCs along with the reference orthorhombic phase of $CsPbBr_3$. The XRD peak of $9S_{CPB}$ is significantly broadened compared to $1S_{CPB}$. (c) Representative TEM image of $1S_{CPB}$ $CsPbBr_3$ NCs having an average size of 8.6 ± 0.7 nm with cubic morphology. (d) Representative TEM image of $9S_{CPB}$ $CsPbBr_3$ NCs having an average size of 3.3 ± 0.4 nm with spherical morphology.

Figure 1a shows the absorbance and PL spectra of the $CsPbBr_3$ NCs synthesized at 170 °C with varied relative supersaturation conditions. $1S_{CPB}$ is termed for reaction conducted in a conventional way ($[PbBr_2]$ =0.03 M) at 170 °C resulting in green emitting $CsPbBr_3$ NCs of size 8-9 nm (Details mentioned in SI). Similarly, $0.5S_{CPB}$, $3S_{CPB}$, $6S_{CPB}$, $9S_{CPB}$, and $12S_{CPB}$ refer to the synthesis of $CsPbBr_3$ NCs where the precursor amount is multiplied by the given factor (0.5, 3, 6, 9, and 12 respectively) while reaction volume is kept constant. With increasing relative supersaturation, the absorbance and PL blueshifts indicating a reduction in average particle size and an increase in quantum confinement. $1S_{CPB}$ has a PL peak at 505 nm which gets blueshifted to 480 nm for reaction conducted under a relative supersaturation condition of $6S_{CPB}$ and further to 462 nm for $9S_{CPB}$. (Figure X1 and X2 in SI shows the variation of PL peak along with corresponding full width at half maxima and PL decay traces of $CsPbBr_3$ NCs synthesized at different relative supersaturation conditions respectively). Figure 1b shows the powder X-ray diffraction (PXRD) pattern of the two $CsPbBr_3$ samples, $1S_{CPB}$ and $9S_{CPB}$. The PXRD peaks of $9S_{CPB}$ are significantly broadened compared to $1S_{CPB}$ indicating its ultra-small size. Figures 1c and 1d show representative transmission electron microscopy (TEM) images for the $1S_{CPB}$ and $9S_{CPB}$ NCs respectively (Figure X3 in SI shows TEM images for $6S_{CPB}$). While $1S_{CPB}$ has cubic morphology with an average size of ~ 8.6 nm, $9S_{CPB}$ has spherical morphology with an average size of ~ 3.3 nm. This is seen by other reports also where smaller size shows spherical morphology indicating stabilization of different high energy facets. The size distribution of $1S_{CPB}$ is found to be 9% while for $9S_{CPB}$ size distribution is found to be ~ 8%, suggesting homogeneous size distribution of particles.

To check the effect of synthesis temperature on the size of $CsPbBr_3$ NCs, $9S_{CPB}$ synthesis is performed at different temperatures, 170 °C, 130 °C, 100 °C and 80 °C. Figure 2a shows the absorption and PL spectra of $9S_{CPB}$ synthesized at different temperatures. (Figure X4 in SI shows PL decay traces of $9S_{CPB}$ synthesized at different temperatures). The spectra do not vary significantly under the various temperature reaction conditions suggesting similar particle sizes for these batches of NCs. This is further corroborated by recording the TEM images of these samples. Figure 2b shows the TEM image of $9S_{CPB}$ synthesized at 80 °C (denoted as $9S_{CPB}$ @80 °C) showing similar size to the $9S_{CPB}$ synthesized at 170 °C (shown in Figure 1d). The size of $CsPbBr_3$ NCs synthesized at higher relative supersaturation is independent of temperature, which is very interesting. Unlike the conventional synthesis of $CsPbBr_3$ NCs, where lowering the temperature reduces the particle size or dimensionality, the size of the NCs remains similar in this case. We hypothesize that at such large relative supersaturation conditions, the range of reaction/growth temperatures investigated in this study has minimal influence in controlling the nucleation and growth of the crystals.

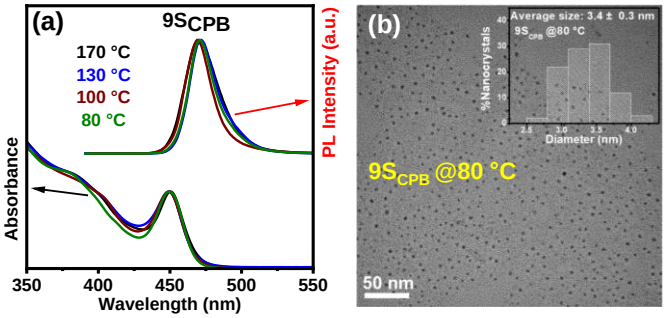

Figure 2: (a) Absorbance and PL spectra of $9S_{CPB}$ $CsPbBr_3$ NCs sample synthesized at different temperatures. The absorbance and PL spectra remain similar at different synthetic temperatures implying similarity in size. (b) Representative TEM image of $9S_{CPB}$ $CsPbBr_3$ NCs synthesized at 80 °C. Inset shows the size distribution of the NCs having an average size of 3.4 ± 0.3 nm and spherical morphology. This is interesting as both $9S_{CPB}$ $CsPbBr_3$ NCs synthesized at 170 °C and 80 °C have similar sizes.

We then proceeded to optimize the reaction conditions including the relative supersaturation concentration and time of reaction (Figure X5 in SI shows the PL spectra of $9S_{CPB}$ @170 °C at different reaction

times) to further fine-tune the PL peak and narrow down the size dispersion. Figure 3a shows the absorbance and PL spectra with the first excitonic peak at 449 nm and corresponding PL peak at 461 nm of the optimized $CsPbBr_3$ NCs sample, $10S_{CPB}$ NCs. The PL peak has a narrow FWHM of 17 nm with a PL quantum yield (QY) of 66 % (Figure X6 in SI shows the determination of PL QY). *Please note that no size-selective precipitation has been used to reduce the particle size dispersion and no post synthetic modifications have been used to boost the PL QYs.* Figure 3b shows the TEM image of the $10S_{CPB}$ NCs with the size distribution. The NCs have spherical morphology with an average size of 3.2 nm.

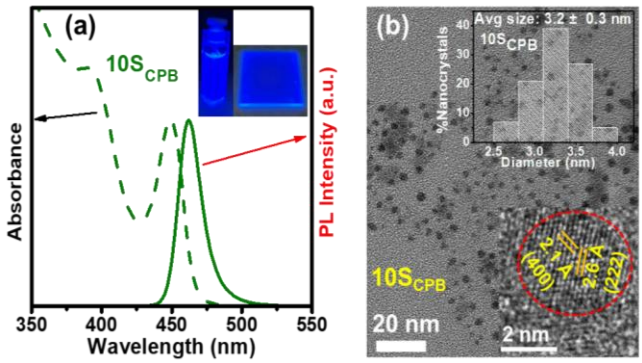

Figure 3: (a) Absorbance and PL spectra of optimized $10S_{CPB}$ NCs having PL peak at 461 nm with PL QY of 66%. Inset shows the digital photograph of the colloidal dispersion of NCs and its thin film on glass under UV light. (b) TEM image of optimized $10S_{CPB}$ $CsPbBr_3$ NCs. Inset shows the size distribution of the NCs with an average size of 3.2 ± 0.3 nm and also the high-resolution TEM image with the lattice planes assigned on an individual NC.

$CsPbBr_3$ NCs synthesized at lower temperature having size < 4 nm or thinner nanoplatelets do exhibit blue emission but these NCs are not spectrally stable and over time they grow in size and their absorption/emission redshifts towards higher wavelengths.[26,27] However, we observe that NCs synthesized by increasing the relative supersaturation condition at elevated temperatures (> 170 °C) do not suffer from this problem and their absorption/emission does not change with storage time. To show this, we synthesized two sets of blue emitting $CsPbBr_3$ NCs; one at a lower temperature (80 °C), termed as $1S_{CPB}$ @80 °C and the other blue emitting sample at increased relative supersaturation condition at a higher temperature, termed as $10S_{CPB}$ @170 °C. Both these samples are then irradiated with UV light (365 nm, 50W), and their absorption and emission spectra are recorded with increasing irradiation time. From Figures 4a and 4b, we can see absorption and emission of $1S_{CPB}$ @80 °C redshifts with increasing time under UV irradiation. The NCs transform from blue emitting to green emitting dots within 3 hours only. This redshift in emission is due to the growth of NCs, as they agglomerate rapidly from smaller to bigger NCs. Figures 4c and 4d shows the TEM images of $1S_{CPB}$ @80 °C before and after the UV irradiation respectively. Note that the growth of these NCs also happens without external UV irradiation but takes a longer time (the growth is more significant for films as shown in Figure X7 in SI).

Similarly, this UV irradiation test is also applied for the $10S_{CPB}$ @170 °C synthesized sample and we see that it is stable under the UV irradiation and absorption/emission does not change with time as shown in Figures 4e and 4f. Figures 4g and 4h show TEM images of the NCs before and after UV irradiation, verifying that their shapes and sizes remain unchanged.

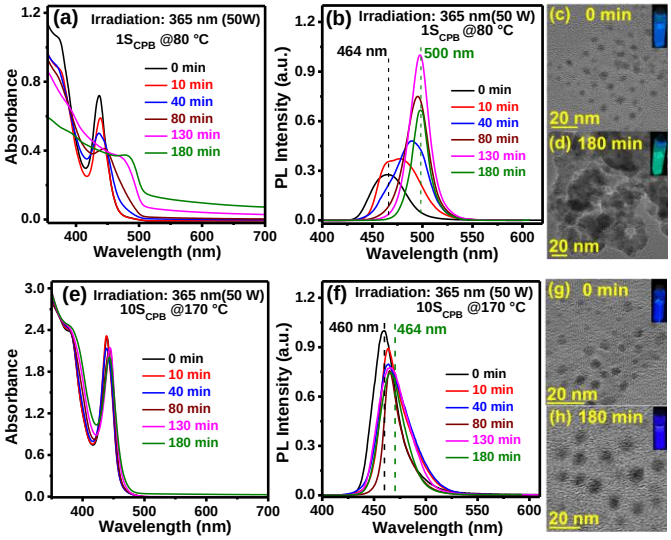

Figure 4: (a) Absorbance and (b) PL spectra of blue emitting sample $CsPbBr_3$ NCs synthesized at a lower temperature, $1S_{CPB}$ @80 °C with varied UV irradiation time. (c, d) TEM image of $1S_{CPB}$ @80 °C before (0 minutes) and after UV irradiation (180 minutes) respectively. Inset shows the photograph of samples where the emission color changed from blue to green. (e) Absorbance and (f) PL spectra of blue emitting sample $CsPbBr_3$ NCs synthesized at a higher temperature at increased relative supersaturation, $10S_{CPB}$ @170 °C with varied UV irradiation time. (g, h) TEM image of $10S_{CPB}$ @170 °C before (0 minutes) and after UV irradiation (180 minutes) respectively. Inset shows the photograph of samples where blue emission is maintained. (Note: min =minutes)

Smaller NCs have high energy facets on their surface and so they tend to grow in size to minimize their free energy. Generally, ligands on the surface of NCs hinder this growth but for perovskite NCs, the ligand binding is weak and dynamic and hence insufficient to stabilize the smaller NCs. Elemental composition determined by energy dispersive spectroscopy (EDS) suggests that $10S_{CPB}$ @170 °C is very deficient in Cs compared to Pb (Table X3 in SI). Although ligand density is similar for both the sample (Figure X8 in SI shows thermogravimetric spectra of the $CsPbBr_3$ NCs), nuclear magnetic resonance (NMR) spectra (Figure X9, X10, and X11 in SI) suggest that the $10S_{CPB}$ @170 °C samples have the signature of oleylammonium (OLA^+) binding. Previous literature has shown that OLA^+ ions bind to $CsPbBr_3$ NCs by substituting Cs^+ ions on the surface.[28] We hypothesize that the $10S_{CPB}$ @170 °C NCs are stabilized by the OLA^+ binding that replaces the Cs^+ ion on the surface of the NCs, which prevents them from growing in size. On the other hand, the $1S_{CPB}$ @80 °C NCs do not have such strong ligand binding, which makes them prone to crystal growth. Based on this observation, we also

hypothesize that there exists a minimum temperature required for OLA^+ to replace the Cs^+ ion on the surface of $CsPbBr_3$ NCs.

In conclusion, we have shown that the size of $CsPbBr_3$ NCs can be controlled and reduced to achieve strongly confined NCs just by increasing the relative supersaturation condition, without changing the ligand nature or the synthesis temperature. We have obtained $CsPbBr_3$ NCs of size ~ 3.2 nm with a high PL QY of around 66% and narrow FWHM of 17 nm without doing any post synthetic modifications. The resulting small NCs are stable against subsequent grain growth and maintain their desired absorption and emission properties even after storage for months (> 6 months). These NCs can thus be used for the fabrication of blue perovskite LEDs where stability and high efficiency remain elusive. A more detailed study about the size control, growth, and surface analysis of these NCs is still required and would be part of our further research.

VKR acknowledges funding from the NYU Mega-Grants Initiative Seed Fund. We also gratefully acknowledge support for instrument use, scientific and technical assistance from the NYU Shared Instrumentation Facility through the Materials Research Science and Engineering Center (MRSEC) and MRI programs of the National Science Foundation under Award numbers DMR-1420073 and DMR-0923251 and the Imaging and Surface Science Facilities of Advanced Science Research Center at the Graduate Center of the City University of New York (CUNY).

Conflicts of interest

There are no conflicts to declare.

Notes and references

1 A. Dey, J. Ye, A. De, E. Debroye, S. K. Ha, E. Bladt, A. S. Kshirsagar, Z. Wang, J. Yin, Y. Wang, et al., *ACS Nano,* 2021, ***15,*** 10775–10981.

2 L. Polavarapu, B. Nickel, J. Feldmann and A. S. Urban, *Adv. Energy Mater.,* 2017, ***7,*** 1700267.

3 K. Lin, J. Xing, L. N. Quan, F. P. de Arquer, X. Gong, J. Lu, L. Xie, W. Zhao, D. Zhang, C. Yan, et al., *Nature,* 2018, ***562,*** 245–248.

4 Y. Hassan, J. H. Park, M. L. Crawford, A. Sadhanala, J. Lee, J. C. Sadighian, E. Mosconi, R. Shivanna, E. Radicchi, M. Jeong, et al., *Nature,* 2021, ***591,*** 72–77.

5 C. -H. Angus Li, Z. Zhou, P. Vashishtha and J. E. Halpert, *Chem. Mater.,* 2019, ***31,*** 6003–6032.

6 Y. Jiang, C. Sun, J. Xu, S. Li, M. Cui, X. Fu, Y. Liu, Y. Liu, H. Wan, K. Wei, et al., *Nature,* 2022, ***612,*** 679–684.

7 Z. Liang, S. Zhao, Z. Xu, B. Qiao, P. Song, D. Gao and X. Xu, *ACS Appl. Mater. Interfaces,* 2016, ***8,*** 28824–28830.

8 L. Protesescu, S. Yakunin, M. I. Bodnarchuk, F. Krieg, R. Caputo, C. H. Hendon, R. X. Yang, A. Walsh and M. V. Kovalenko, *Nano Lett.,* 2015, ***15,*** 3692–3696.

9 V. K. Ravi, A. Swarnkar, R. Chakraborty and A. Nag, *Nanotechnology,* 2016, ***27,*** 325708.

10 X. Li, Y. Wu, S. Zhang, B. Cai, Y. Gu, J. Song, and H. Zeng, *Adv. Funct. Mater.,* 2016, **26,** 2435–2445.

11 J. A. Sichert, Y. Tong, N. Mutz, M. Vollmer, S. Fischer, K. Z. Milowska, R. García Cortadella, B. Nickel, C. Cardenas-Daw, J. K. Stolarczyk, et al., *Nano Lett.,* 2015, ***15,*** 6521–6527.

12 Q. A. Akkerman, S. G. Motti, A. R. Srimath Kandada, E. Mosconi, V. D'Innocenzo, G. Bertoni, S. Marras, B. A. Kamino, L. Miranda, F. de Angelis, et al., *J. Am. Chem. Soc.,* 2016, ***138,*** 1010–1016.

13 J. Shamsi, Z. Dang, P. Bianchini, C. Canale, F. di Stasio, R. Brescia, M. Prato and L. Manna, *J. Am. Chem. Soc.,* 2016, ***138,*** 7240–7243.

14 Q. A. Akkerman, T. P. T. Nguyen, S. C. Boehme, F. Montanarella, D. N. Dirin, P. Wechsler, F. Beiglböck, G. Rainò, R. Erni, C. Katan, et al., *Science,* 2022, ***377,*** 1406–1412.

15 Y. Xu, Q. Zhang, L. Lv, W. Han, G. Wu, D. Yang, and A. Dong, *Nanoscale,* **2017,** 9, 17248-17253.

16 K. Xu, A. C. Allen,- B. Luo, E. T. Vickers, Q. Wang, W. R. Hollingsworth, A. L. Ayzner, X. Li, and J. Z. Zhang, *J. Phys. Chem. Lett.,* **2019,** 10, 4409-4416.

17 B. Shu, Y. Chang, E. Xu, S. Yang, J. Zhang, Y. Jiang, X. Cheng, and D. Yu, *Nanotechnology,* **2021,** 32, 145712.

18 C. F. Todd, and J. Z. Zhang, *J. Phys. Chem. Lett.,* **2023,** 14, 10630-10633.

19 D. A. Idosa, M. Abebe, D. Mani, A. Thankappan, S. Thomas, F. G. Aga, and J. Y. Kim, Photonics, 2023, 10, 802.

20 Y. Chen, S. Lu, M. Nan, J. Xie, W. Shen, A. N. Aleshin, G. Cheng, S. Chen, and W. Huang, *Adv. Optical Mater.,* **2023,** 11, 23004773.

21 A. Priyam, S. Ghosh, S. C. Bhattacharya and A. Saha, *J. Colloid Interface Sci.,* 2009, ***333,*** 195–201.

22 I. Kumar, A. Priyam and R. K. Choubey, *AIP Conf. Proc.,* 2013, ***1536,*** 231–232.

23 I. V. Markov, *Crystal Growth for Beginners: Fundamentals of Nucleation,* Crystal Growth and Epitaxy; 2nd ed.; World Scientific: Singapore; River Edge, N.J., 2003

24 H. Lin, Z. Lei, Z. Jiang, C. Hou, D. Liu, M. Xu, Z. Tian and Z. Xie, *J. Am. Chem. Soc.,* 2013, ***135,*** 9311–9314.

25 S. Patra, B. Bhushan, and A. Priyam, *Dalton Trans.,* **2016,** 45, 3918-3926.

26 Y. Bekenstein, B. A. Koscher, S. W. Eaton, P. Yang and A. P. Alivisatos, *J Am. Chem. Soc.,* 2015, ***137,*** 16008–16011.

27 H. Zhu, Z. Liu, C. Xu, C. Chen, J. Wen, K. Yang, S. Chen and Y. Pan, *J. Alloys Compd.,* 2022, ***923,*** 166322.

28 V.K. Ravi, P. K. Santra, N. Joshi, J. Chugh, S. K. Singh, H. Rensmo, P. Ghosh and A. Nag, *J. Phys. Chem. Lett.,* 2017, ***8,*** 4988–4994.